Chiral Symmetry and Threshold π^0 Electroproduction

Véronique Bernard
Centre de Recherches Nucléaires et Université Louis Pasteur de Strasbourg, Physique Théorique, BP 20Cr, 67037 Strasbourg CEDEX 2, France

Norbert Kaiser
Physik Department T30, Technische Universität München, James Franck Strasse, D-8046 Garching, Germany

T.-S. H. Lee
Physics Division, Argonne National Laboratory, Argonne, Illinois 60439

Ulf-G. Meissner
Universität Bern, Institut für Theoretische Physik, Sidlerstrasse 5, CH-3012 Bern, Switzerland
(Received 14 October 1992)

The electroproduction of neutral pions off protons close to threshold is studied within the framework of chiral perturbation theory. We compare to the recent data from NIKHEF and find good agreement. Further measurements as tests of chiral symmetry are discussed.

PACS numbers: 13.60.Le, 11.40.Fy

Threshold pion photo- and electroproduction off protons allows us to test our understanding of the strong interactions at low energies, i.e., in the nonperturbative regime. In the last few years, extensive data were obtained for the photoproduction process $\gamma+p\to\pi^0+p$ at Saclay [1] and Mainz [2]. This led to numerous investigations concerning the so-called low-energy theorem (LET) for the electric dipole amplitude E_{0+} at threshold [3,4] and also a critical reanalysis of the data was performed [5–8]. Furthermore, in QCD the LET was reconsidered and it was found that there are additional terms in the expansion of E_{0+} in powers of $\mu=M_\pi/m$ (ratio of the pion to the nucleon mass) at next-to-leading order μ^2 [9,10]. This effect is due to a nonanalyticity in the quark mass whose origin is the triangle diagram. New experimental information has recently become available for the electroproduction process $\gamma^*+p\to\pi^0+p$, where γ^* denotes the virtual photon [11]. The data were obtained in the energy range from 0 to 2.5 MeV above production threshold and photon four-momenta squared (k^2) between -0.04 and -0.1 GeV$^2/c^2$. This experiment is a major step beyond previous measurements which were characterized by a poor energy resolution and also did not come close enough to threshold; i.e., they were dominated by the M_{1+} multipole. The aim of our Letter is to confront low-energy QCD predictions with these new data and to propose further measurements which are sensitive to the chiral sector of QCD.

Our calculation is based on the chiral perturbation theory (CHPT) formulation developed in Refs. [9,10]. The essential ingredients of CHPT can be briefly summarized as follows. At low energies, the strong interactions are dictated by the spontaneously broken chiral symmetry. In the chiral limit of vanishing quark masses the pseudoscalar Goldstone bosons are massless. Their self-interactions and interactions with other particles (e.g., the nucleon) are severely constrained by the Ward-Takahashi (WT) identities of the broken chiral symmetry and by Goldstone's theorem. In fact, the WT identities can be solved in a systematic fashion by making use of an effective field theory which consists of a string of terms with an increasing number of derivatives and quark mass insertions. For the $\pi N\gamma$ system we consider here, the lowest-order term is of order q (one derivative) and contains a few parameters like the pion decay constant (F_π) or the axial-vector coupling (g_A) (in the chiral limit). Calculating tree diagrams with the lowest-order effective Lagrangian is not sufficient since unitarity is violated. This can be cured in a perturbative fashion by going at next-to-leading order and considering loops [12]. At this order, one also has a set of higher derivative local terms. These are accompanied by *a priori* unknown coefficients, the so-called low-energy constants. Since in general the pion loop diagrams are divergent, one has to perform an order-by-order renormalization procedure. The infinities can be absorbed in the low-energy couplings. The remaining finite pieces of the various low-energy constants can be determined from phenomenology [13] or estimated by the exchange of heavy meson resonances [14]. A general discussion of these aspects in the $\pi N\gamma$ system is given in Refs. [15,16].

Apart from well-known lepton kinematical factors, the $p(e,e'\pi^0)p$ cross section is determined from the amplitude of the process $\gamma^*(k)+p(p_1)\to\pi^0(q)+p(p_2)$ with $k^2<0$. Within CHPT, the transition amplitude takes the form

$$T(\gamma^*p\to\pi^0p)=T^{(\text{tree})}+T^{(1\text{-loop})}+T^{(\text{c.t.})}, \qquad (1)$$

where $T^{(\text{tree})}$ is the lowest-order amplitude generated from tree graphs of the nonlinear σ model coupled to nucleons. One should notice that the tree amplitude does not contain form factors or the anomalous magnetic mo-

ment of the proton. At next-to-leading order, one has contributions from loops and counterterms (c.t.). In the case under consideration, there are three finite counterterms up to and including dimension q^3 related to photon couplings. These read

$$\mathcal{L}_{\pi N}^{\text{c.t.}} = d_1 \epsilon_{\mu\nu\alpha\beta} \bar{\Psi} \gamma^\mu u^\nu F_+^{\alpha\beta} \Psi + \tilde{c}_6 \bar{\Psi} \sigma_{\mu\nu} F_+^{\mu\nu} \Psi + \tilde{b}_9 \bar{\Psi} \gamma_\mu D_\nu F_+^{\mu\nu} \Psi , \quad (2)$$

with $u_\mu = iu^\dagger \nabla_\mu U u^\dagger$ and $u = \sqrt{U}$. The matrix-valued field U collects the pion fields in a nonlinear representation. We work in flavor SU(2) in the isospin limit and use the σ-model gauge $U = (\sigma + i\tau \cdot \pi)/F_\pi$ subject to the constraint $\sigma^2 + \pi^2 = F_\pi^2$. $F^{\mu\nu}$ is the conventional photon field strength tensor and $F_{\mu\nu}^+ = u^\dagger Q F_{\mu\nu} u + u Q F_{\mu\nu} u^\dagger$, with Q the nucleon charge matrix. The covariant derivative contains external vector and axial-vector fields, i.e., it gives the coupling of the photon to the nucleons and pions. The first term in (2) has already been discussed in the photoproduction calculation [16] and the coefficient d_1 was estimated from resonance exchange. The second and third terms are necessary to account for the physical values of the anomalous magnetic moment and the electric charge radius of the proton, respectively. It is important to notice that the anomalous magnetic moment κ_p and the form factors are built up order by order from the loops and counterterms. Also, by construction, gauge invariance is preserved. To calculate the transition amplitude [Eq. (1)], one expands in terms of a set of gauge- and Lorentz-invariant functions [17]

$$T^\mu = i\bar{u}(p_2) \gamma_5 \sum_{i=1}^{6} M_i^\mu A_i(s,u,k^2) u(p_1) , \quad (3)$$

where the M_i^μ can be found in Ref. [17], $s = (p_1 + k)^2$, $u = (p_1 - q)^2$, and the A_i will be calculated in chiral perturbation theory. To one-loop order, the contributions to the A_i fall into three separately gauge-invariant subsets of diagrams. The explicit form of the first of these sets is given in [10] and that of the other two will be given elsewhere [18]. The second class of diagrams essentially builds up the anomalous magnetic moment and the proton electromagnetic form factors and the third one contains the so-called box graphs. Obviously, in the photoproduction case $k^2 = 0$ one recovers the results of Ref. [16]. To compare with the data of Ref. [11], we have to calculate the triple differential cross section of the reaction $p(e,e'\pi^0)p$ from the amplitude defined in Eq. (3). In terms of the S- and P-wave multipoles, it can be cast into the following form [19]:

$$\frac{d^3\sigma}{d\Omega_e dE_e} = 4\pi\Gamma \frac{|\mathbf{q}_\pi^*|}{k_L} \frac{W}{m} \{a_0 + b|\mathbf{q}_\pi^*|^2\} , \quad (4)$$

with Γ the virtual photon flux factor, $\mathbf{q}_\pi^*$ the pion three-momentum in the πN frame, $k_L = (s - m^2)/2m$ the equivalent real photon energy, m the proton mass, and $W = \sqrt{s}$ the invariant energy. The second term proportional to b in Eq. (4) contains the contributions from the P-wave multipoles. The focus of the current interest is the first term a_0 which depends only on the S-wave multipoles E_{0+} and L_{0+}:

$$a_0 = |E_{0+}|^2 - \epsilon \frac{k^2}{k_0^{*2}} |L_{0+}|^2 , \quad (5)$$

where ϵ and $k_0^* = (s - m^2 + k^2)/2\sqrt{s}$ represent, respectively, a measure of the transverse linear polarization and the energy of the virtual photon in the πN frame. In Ref. [11], a_0 was extracted from the data with an unprecedented accuracy.

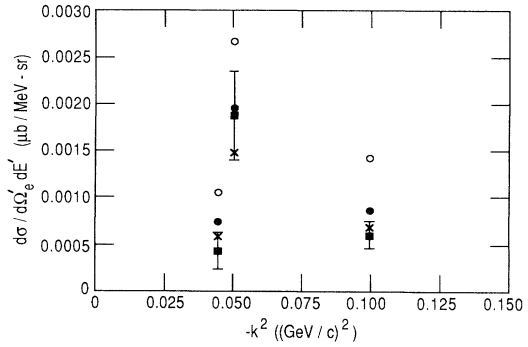

FIG. 1. Comparison of the NIKHEF data [11] with the predictions from one-loop CHPT (×), tree-level (open circles), and PV (solid circles) calculations.

Let us now confront the chiral one-loop predictions with the data. We compare in Fig. 1 the CHPT predictions (marked as ×) and the data from NIKHEF [11]. In the same figure we also show the results from tree diagrams (open circles) and from the pseudovector (PV) Born terms with form factors (solid circles) as explicitly specified by model B of Nozawa and Lee [19]. Note that all of the PV results presented here do not include the vector-meson-exchange and final-state-interaction terms introduced in Ref. [19] since they induce a strong model dependence. The possible connection between these two effects and CHPT will be investigated elsewhere [18]. We see that the one-loop diagrams drastically reduce the calculated cross sections and bring the CHPT results within the experimental uncertainties. The results from PV Born terms are, however, also not too different from the data. To have a rigorous test of CHPT, more precise measurements are clearly needed. Let us now focus our attention on the k^2 dependence of various $p(e,e'\pi^0)p$ cross sections. We consider a kinematics with $W = 1074$ MeV, which is perhaps the most realistic case for the experiments in the near future. At this near threshold energy, $W_{\text{thr}} = 1073.26$ MeV, the S-wave multipoles dominate. In Fig. 2, the S-wave cross section defined in Eq. (5) is displayed ($\epsilon = 0.58$). The prediction of Scherer and Koch [20] is very similar to that of the PV terms. Notice that the data of Ref. [11] also shown are obtained for

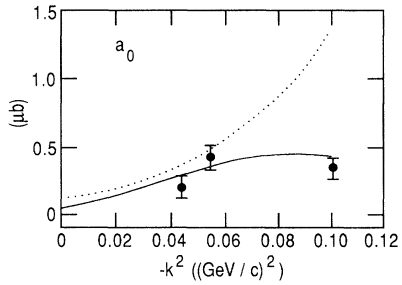

FIG. 2. The S-wave components of the cross sections, calculated from CHPT (solid line) and PV (dotted line) are compared. The kinematics is $W=1074$ MeV and $\epsilon=0.58$. The data extracted in Ref. [11] are also shown.

$\epsilon=0.58$, 0.79, and 0.62, in order. However, the CHPT prediction for $\epsilon=0.79$ lies only slightly above the solid line shown in Fig. 2. The overall agreement between the data and the CHPT prediction is satisfactory (see, however, discussion below). Clearly, the differences between CHPT and PV can be distinguished easily in the region near $k^2=-0.1$ GeV$^2/c^2$. The most effective way to test the CHPT predictions is to perform experiments which allow a separation of the longitudinal and transverse parts of the cross section since they have a very different k^2 dependence. Furthermore, they are drastically different from the predictions based on the PV terms.

We have also explored the k^2 dependence of various π^0 differential cross sections (as defined in Ref. [19]). Here we only present in Fig. 3 the results for the transverse differential cross sections, which call for an experimental test. The most striking feature is that the CHPT predictions become forward peaked as $|k^2|$ becomes larger than 0.04 GeV$^2/c^2$, while the PV results remain backward peaked until $|k^2|\simeq 0.07$ GeV$^2/c^2$. This is illustrated in Fig. 3. For comparison, in the shapes of longitudinal differential cross sections one finds no striking differences. It is important to notice that the transverse cross sections (cf. Fig. 3) contain contributions from P-wave multipoles. Although these multipoles are small, they can significantly contribute to the cross section through their interferences with the S-wave multipoles. There are pronounced differences in all multipoles between the CHPT and PV predictions (for details, see Ref. [18]). Therefore, to have a good test of CHPT it is not sufficient to compare the CHPT prediction for the S-wave multipoles (cf. Fig. 2) with the data since in the latter case the P-wave contribution was taken from some other sources or by extrapolating existing analyses at higher energies to threshold via a Born series. In the future, it will be preferable to compare the theoretical predictions of the cross sections directly with the measurements.

To summarize, we have performed a calculation of threshold pion electroproduction in the framework of chiral perturbation theory. We have shown that loop effects are necessary to understand the recently measured

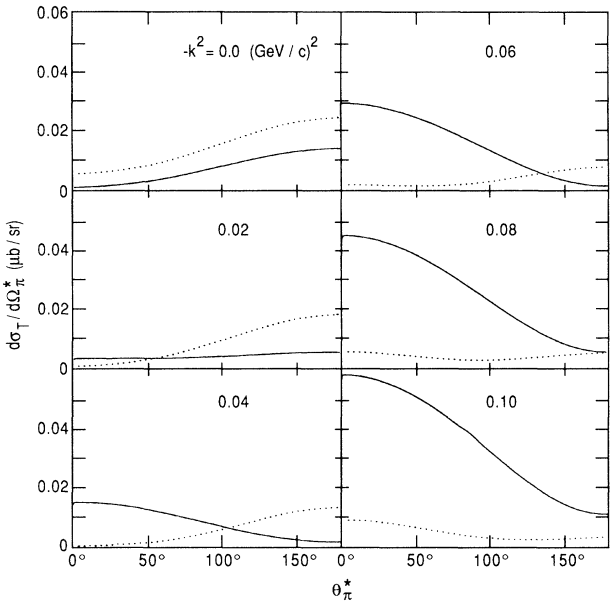

FIG. 3. The k^2 dependence of the π^0 transverse differential cross sections in the final πN center-of-mass system (as defined in Ref. [19]) calculated from CHPT (solid curves) and PV (dotted curves) are compared. The kinematics is $W=1074$ MeV and $k^2=0,\ldots,0.1$ (GeV/c)^2.

triple differential cross section close to threshold and at photon four-momentum squared between -0.04 and -0.1 GeV$^2/c^2$. However, we have also stressed that more precise measurements, in particular of the transverse cross sections, are needed to serve as a test of chiral perturbation theory. On the theoretical side, further investigations of higher loop effects are definitively needed to learn about the convergence of the chiral expansion and to estimate the influence of degrees of freedom not present in the one-loop calculation presented here [21]. A more detailed account of this topic and also the discussion of charged pion electroproduction at threshold [22] will be given in Ref. [18].

We are grateful to Pat Welch for providing us with the NIKHEF data before publication. This work was supported in part by funds provided through the Deutsche Forschungsgemeinschaft under Contract No. ME864/2-2, by Schweizerischer Nationalfonds, and by the U.S. Department of Energy, Nuclear Physics Division, under Contract No. W-31-109-ENG-38. U.-G.M. is a Heisenberg fellow.

[1] E. Mazzucato *et al.*, Phys. Rev. Lett. **57**, 3144 (1986).
[2] R. Beck *et al.*, Phys. Rev. Lett. **65**, 1841 (1990).
[3] I. A. Vainshtein and V. I. Zakharov, Nucl. Phys. **B36**, 589 (1972).

[4] P. de Baenst, Nucl. Phys. **B24**, 633 (1970).
[5] R. Davidson and N. C. Mukhopadhyay, Phys. Rev. Lett. **60**, 748 (1988).
[6] A. M. Bernstein and B. R. Holstein, Comments Nucl. Part. Phys. **20**, 197 (1991).
[7] J. Bergstrom, Phys. Rev. C **44**, 1768 (1991).
[8] S. Nozawa, T.-S. H. Lee, and B. Blankleider, Phys. Rev. C **41**, 213 (1991); **41**, 1306 (1991).
[9] V. Bernard, J. Gasser, N. Kaiser, and Ulf-G. Meissner, Phys. Lett. B **268**, 291 (1991).
[10] V. Bernard, N. Kaiser, and Ulf-G. Meissner, Phys. Lett. B **282**, 448 (1992).
[11] T. P. Welch *et al.*, Phys. Rev. Lett. **69**, 2761 (1992); T. P. Welch (private communication).
[12] S. Weinberg, Physica (Amsterdam) **96A**, 327 (1979).
[13] J. Gasser and H. Leutwyler, Ann. Phys. (N.Y.) **158**, 142 (1984).
[14] G. Ecker, J. Gasser, A. Pich, and E. de Rafael, Nucl. Phys. **B321**, 311 (1989); J. F. Donoghue, C. Ramirez, and G. Valencia, Phys. Rev. D **39**, 1947 (1989).
[15] J. Gasser, M. E. Sainio, and A. Švarc, Nucl. Phys. **B307**, 779 (1988).
[16] V. Bernard, N. Kaiser, and Ulf-G. Meissner, Nucl. Phys. **B383**, 442 (1992).
[17] F. A. Berends, A. Donnachie, and D. L. Weaver, Nucl. Phys. **B4**, 1 (1967).
[18] V. Bernard, N. Kaiser, T.-S. H. Lee, and Ulf-G. Meissner (to be published).
[19] S. Nozawa and T.-S. H. Lee, Nucl. Phys. **A513**, 511 (1990).
[20] S. Scherer and J. H. Koch, Nucl. Phys. **A534**, 461 (1991).
[21] V. Bernard, N. Kaiser, and Ulf-G. Meissner, "Testing Nuclear QCD: $\gamma p \to \pi^0 p$ at Threshold," πN Newsletter No. 7 (to be published). There it was shown that isospin breaking (in the class I diagrams) can lead to sizable corrections, e.g., a strong cusp effect in the electric dipole amplitude E_{0+}.
[22] V. Bernard, N. Kaiser, and Ulf-G. Meissner, Phys. Rev. Lett. **69**, 1877 (1992).